Saccadic suppression as a perceptual consequence of efficient sensorimotor estimation

F. Crevecoeur[1,2], K. P. Kording[3]

[1]*Institute of Information and Communication Technologies, Electronics and Applied Mathematics (ICTEAM), Université catholique de Louvain (UCLouvain), Belgium*
[2] *Institute of Neuroscience (IoNS), UCLouvain*
[3]*Rehabilitation Institute of Chicago, Northwestern University, Chicago, USA*

Corresponding Author:
K. P. Kording, 345 E Superior St., Rm. 1479
Chicago, IL, 60611, USA
Tel.: 1-312-238-6966
E-mail: kk@northwestern.edu

Acknowledgements

41 **Abstract**

42 Humans perform saccadic eye movements two to three times per second. When doing so, the

43 nervous system strongly suppresses sensory feedback for extended periods of time in comparison with

44 the movement time. Why does the brain discard so much visual information? Here we suggest that

45 perceptual suppression may arise from efficient sensorimotor computations, assuming that perception

46 and control are fundamentally linked. More precisely, we show that a Bayesian estimator should reduce

47 the weight of sensory information around the time of saccades, as a result of signal dependent noise and

48 of sensorimotor delays. Such reduction parallels the behavioral suppression occurring prior to and during

49 saccades, and the reduction in neural responses to visual stimuli observed across the visual hierarchy.

50 We suggest that saccadic suppression originates from efficient sensorimotor processing, indicating that

51 the brain shares neural resources for perception and control.

Introduction

People skillfully combine acquired knowledge, and sensory feedback, a combination that is typically modeled using Bayesian statistics [1,2]. This framework effectively captures behavior in numerous tasks broadly corresponding to perceptual decision-making [3-7], or online movement control [8-11]. Although perceptual decision-making and sensorimotor control are often considered different phenomena, they cannot really be dissociated in the real world – we need to use the same brain for movement and perception [12,13]. Perceptual decision-making and sensorimotor behaviors may thus be linked.

A salient case of crosstalk between perception and sensorimotor behavior is *saccadic suppression*: visual acuity is reduced around the time of a saccade. It is often assumed that this mechanism maintains stable perception of our surroundings [14]. However, the behavioral and neural dynamics of saccadic suppression are difficult to explain if it were purely related to compensating for movement-related effects.

Indeed, previous work has shown that saccadic suppression is controlled centrally, and typically lasts for >100ms even for saccadic movements of ~50ms [15]. Furthermore, simulating the displacement of the retinal image without a saccade does not elicit similar suppression as during real saccades [16,17]. As well, the reduction of visual acuity was reported to selectively impact the neural pathways contributing to motion perception (i.e., the magnocellular stream), without complete suppression [18], while leaving information with high frequency contents or color unaffected [19,20]. It is unclear why maintaining perceptual stability would require such a long, powerful, and selective suppression of sensory feedback, if it were purely related to perception, and independent of motor control (Fig. 1, separate resources hypothesis, H1). After all, there is a price to be paid to discard so much sensory information for some 100ms. Thus, saccadic suppression is a complex phenomenon, for which a meaningful function has not been clearly identified.

3

75   Here we phrase this problem as a problem of shared resources – the same neural hardware is

76   used for sensorimotor tasks and perceptual decision-making (Fig. 1, shared resources, H2). Formulating

77   this problem in the framework of Bayesian estimation, we show theoretically that several features of

78   saccadic suppression are expected if the brain uses the same posterior beliefs about the state of the eye

79   for perception and control. Our model shows that uncertainty about the instantaneous state of the eye

80   should increase with motor commands as a result of signal-dependent noise and of sensorimotor delays,

81   making delayed sensory information less reliable around the time of movement. In an optimal

82   estimation framework, this gives lower weights to sensory inputs when we move. Our study thus shows

83   how sensorimotor control can give rise to sensory suppression in an efficient brain, provided that neural

84   resources are shared between perception and control.

Results

85

An optimal control model of eye movements

86

87   If we want to explore the relationship between saccadic suppression and control we need to

88   model the underlying system. First, the nature of the representation matters: although saccades are

89   often simplistically viewed as ballistic (or *open-loop*) movements, these movements are monitored

90   online through the corollary discharge [21-25]. Second, sensory feedback matters: we are not "blind" during

91   saccades. There is no peripheral interruption of sensory inflow, and information about specific

92   spatiotemporal frequency or color is still good [19,26]. Moreover, target jumps during long saccades can

93   influence movement [27,28]. We should thus model saccades as driven by closed-loop control (Fig. 2a).

94   To describe saccades in the context of closed loop control, we model a controller that takes the

95   sensory feedback and the corollary discharge as input, and outputs motor commands. We employ a

96   Linear-Quadratic-Gaussian (LQG) controller, which can deal with noise both in sensory feedback and

97   control signals. As model for the oculomotor plant we use a second order model (see Methods). This

98   explicit model of saccadic control allows us to derive predictions of eye movement behaviors and gives

99   us a control process that we can relate to saccadic suppression.

100   The important feature of this control design in the context of this paper is its state estimator. The

101   control of saccadic eye movements relies on the corollary discharges as well as on sensory feedback,

102   which jointly allow state estimation. This state estimator has two main components. The first is a

103   forward model that dynamically updates the current estimate based on the corollary discharge (Fig. 2a,

104   bottom: Forward Model). The output is a prior estimate of the next state at the next step. The second

105   component is the sensory extrapolation, which combines the delayed sensory feedback with the

106   corollary discharge to estimate the current state (Fig. 2a: Sensory Extrapolation, red). This sensory

107   extrapolation is critical for the behavior of the model.

108   The presence of sensory extrapolation is supported by previous studies showing that error

109   signals used to generate saccades depend on an estimate of the current state of the eye or of the target

110   [29-33], which clearly requires extrapolation of sensory feedback. Indeed, because the system only has

111   access to the delayed feedback, this feedback must be extrapolated prior to compare it with the one-

112   step prediction, or prior. This operation does not appear explicitly in standard control models in which

113   sensorimotor delays were considered[10,11,34,35], because these previous studies used system

114   augmentation, and the sensory extrapolation in this case falls out of the block-structure of the model.

115   However, this component is necessary, and ignoring it can lead to instability [35]. In the present model, this

116   sensory extrapolation is performed explicitly (Eqn. 5), which also allows incorporating the impact of

117   signal-dependent noise in the extrapolation (see also Methods). The model can then correct the one step

118   prediction, weighting the difference between feedback and expected feedback optimally (Fig. 2a, $K(t)$ is

119   the Kalman gain).

120

121   *Saccades and smooth pursuit*

122   The first behavior that our model must describe is a saccade. The model reproduces stereotyped,

123   step-like trajectory (Fig. 2b, top), like those found during real saccades. Moreover, the associated

124   commands presents with a typical wide agonist burst, followed by short and sharper antagonist activity

125   that stabilizes the eye at the goal target (Fig. 2b, bottom). This pattern of control, shaped by the fast time

126   constants of the oculomotor plant, is compatible with the pattern of burst neurons that generate

127   saccades [21]. Thus the model replicates both behavioral and physiological aspects of saccadic eye

128   movements.

129   A second behavior that our model can capture is smooth pursuit. We do not imply that these two

130   behaviors are supported by the same neural hardware, and the model does not make any prediction

131   about their neural implementation. Instead, we simply assume that optimal state estimation underlies

132   both saccades and pursuit, which is in agreement with the hypothesis that these movements are distinct

133   outputs of shared sensorimotor computations [36,37]. The model reproduces typical responses to changes

134   in target velocity, occurring with or without initial target jump (Fig 2c). When the target starts moving

135   (velocity jump), position error accumulates over the delay interval, which in turn requires a rapid

136   compensatory movement to catch up with the target (Fig. 2b, light blue). Although the controller was

137   not explicitly designed to model the interaction between saccades and pursuit, the catch-up saccade in

138   Fig. 2b naturally falls out of the simultaneous correction for errors both in position and velocity. In

139   contrast, when the target jumps backwards at the onset of the velocity jump (Fig. 2c, dark blue), the eye

140   starts moving smoothly and there is no catch-up saccade [38]. The model also reproduces corrections

141   following perturbations applied during movement through internal monitoring of the corollary discharge,

142   as well as online corrections for target jumps occurring during long saccades (simulations not shown). In

143   all, the model generates typical trajectories and control commands associated with eye movements, and

144   reproduces the dynamic estimation of the target resulting from the sensory extrapolation.

145

146   *Saccadic Suppression as a Consequence of Optimal Estimation*

147   Our muscles produce signal dependent noise; the stronger the muscles pull, the more noisy the

148   state. The phasic activity associated with the agonist burst induces a peak in the variance of the control

149   signal (Fig. 3a, solid). Thus motor commands produce instantaneous noise, and because of the delay,

150   there is no way for the nervous system to directly subtract or filter out this noise. As a consequence, the

151   extrapolation error computed over an interval that includes even a fraction of the control burst has

152   higher variance. In other words, moving the eye effectively induces visual uncertainty, which can only go

153   back to baseline after the end of muscle activation.

154   The time-varying variance induced by control-dependent noise has a direct impact on the

155   importance of visual inputs, through the Kalman gains (Fig. 3b). As the Kalman gain is inversely

156 proportional to the extrapolation variance (see Methods, Eqn. 8), the transient increase in the variance

157 of sensory extrapolation generates a reduction in the weight of sensory feedback about the eye position.

158 And indeed, sensory suppression is seen around the time of simulated saccades (Fig. 3b). The period of

159 suppression is long because high variance period includes the movement time, but also the delay (gray

160 rectangle in Fig. 3c). The model thus predicts that feedback about stimuli from this time window should

161 be given less weight in order to optimally estimate the state of the eye.

162 We can also see related effects in the simulated pursuit task. The presence of a catch up saccade,

163 even a small one (4deg), is sufficient to evoke a transient increase in extrapolation variance (Fig. 3d-f).

164 This results in a reduction in the weight of sensory feedback. In contrast, when the eye starts moving

165 smoothly (Fig. 3f), there is no catch-up saccade needed and the model predicts no visible change in the

166 weight of sensory feedback. The behavioral finding[39] that saccades but not smooth pursuit elicit

167 suppression of sensory feedback, and that the suppression scales with the amplitude of the catch-up

168 saccade, directly results from this model.

169 Thus far, we have described how an efficient state estimator should reduce the weight of

170 sensory feedback around the time of saccade. However, saccadic suppression clearly impacts perception,

171 and it is not obvious how this phenomenon relates to our model. In the introduction we set up two

172 hypotheses. Perception and action could be separate, and in this case the Kalman filter for movement

173 should not affect perception (Fig 1, H1). Alternatively they could share resources, such that a lower

174 Kalman gain for movement should carry through to a lower weight of vision for any estimate, including

175 perceptual ones (Fig 1, H2). If H1 is true, then we should find that both neural and behavioral variables

176 that relate to perception are unaffected by saccades, beyond the limited effect induced by the rapid

177 change of the retinal image [16]. If H2 is true, on the other hand, we should find suppression not only of

178 behavioral variables but also directly in the neural activities associated with sensorimotor control.

179   Behaviorally, we can analyze data from perception experiments. Suppression should occur prior

180   to movement onset, reach a maximum close to movement onset (Fig. 4b), and scale with the movement

181   amplitude with relatively invariant timing across amplitudes. Interestingly, this goes even down to the

182   level of microsaccades, inducing partial suppression despite being very small in amplitude [40]. These

183   known properties of saccadic suppression are in line with the model prediction (Fig. 4b, black): contrasts

184   sensitivity is reduced and visual stimuli such as flashes, gratings, or small displacements are less likely to

185   be accurately perceived [16,19,20,41-43]. This even happens when the stimuli are chosen so that the eye

186   movement does not change the retinal image, which is compatible with the model (see the simulated

187   contrast reduction of a white stripe, Fig. 4a). Finally, although timing is preserved across amplitudes [15],

188   the model predicts that the magnitude of suppression scales with the saccade amplitude as observed

189   experimentally [44]. This is a direct consequence of signal-dependent noise. Hence, the behavioral data is

190   consistent with Hypothesis 2 where sensorimotor behavior and perception share a common neural

191   resource.

192   There is an indirect but interesting parallel between the model's behavior and the selective

193   suppression of stimuli with low frequency contents [19,20]. The model predicts that sensory feedback about

194   the eye position, but not necessarily velocity, should be reduced. The reason is that the expected signal-

195   dependent noise directly impacts the prediction of the forward model about velocity (which is not the

196   case for position given the current estimates of velocity). Because the predicted and extrapolated

197   velocities are both uncertain, the best strategy is to give them similar weights. This is interesting because

198   changes in velocity typically have higher frequency contents than changes in position, thus a selective

199   suppression of stimuli with low frequency contents may be directly related to the reduction in the weight

200   of feedback about position, but not velocity.

201   Neurally, we may also expect changes. One obvious way how changes in Kalman gains could be

202   implemented is that neurons could just be driven less strongly when there is more uncertainty. This

203   should predict reduced firing rates around the time of the saccade. Indeed, a large number of

204   experimental studies have found such a neural suppression across the hierarchy of visual areas [45]. It

205   starts with the lateral geniculate nucleus (LGN) [46] and the superior colliculus (SC) [40], via V1 [47], MT, MST,

206   MSTd [45,48], all the way up to area VIP [48] (Fig 4b, colored). Interestingly, the timing is very similar across

207   brain regions, which emerges naturally from the fact that the loop through the outside world with its

208   delays is the dominating timescale. As predicted by the shared resources model, there is suppression

209   across the entire visual hierarchy.

Discussion

210

211   We have presented a feedback control model that assumes movement dependent-noise and

212   delays, and uses state estimation to optimally control eye movements. It is built on the insight that

213   motor noise is unavoidable and produces sensorimotor uncertainty. It assumes that perception and

214   movement share common resources and hence a common gain on visual input. Behaviorally, it describes

215   the dynamics of both smooth pursuit and saccades. Perceptually, it describes the suppression of

216   sensation around the time of saccades. Neurally, it captures the reduction of neural responses to visual

217   stimuli presented before or during saccades.

218   A clear limitation of our model is that it is difficult to test experimentally. However the important

219   motivation behind this study was that maintaining a stable visual scene, as commonly assumed, does not

220   explain the phenomenon of saccadic suppression. Indeed, suppression in this case should only occur

221   when the eye moves, and should not be stronger than the moderate loss in performance associated with

222   simulated saccades [16]. All discarded information beyond movement-related effects would otherwise

223   represent a net loss (up to ~100ms for some brain areas, Fig. 4b). Thus it is clear that saccadic

224   suppression is either very inefficient, or that maintaining a stable visual scene is just not its only purpose.

225   We provide an alternative explanation that captures suppression qualitatively in the context of

226   sensorimotor control. Rather than providing a definite answer to why suppression occurs, we highlight a

227   plausible explanation and expect that it provide an insightful framework for interpreting data about

228   visual processing.

229   In addition to capturing the major aspects of behavioral and neural suppression, our model

230   explains the previous findings of Watson and colleagues [41], who investigated the detection of noisy

231   gratings in human, and found that the best explanation for saccadic suppression was a stimulus-

232   independent reduction in the response gain. This result is a key aspect of saccadic suppression: the

233   retinal images do not become intrinsically noisier; instead it is the visual system that responds less to a

11

234   given stimulus. Our model also accounts for this result: by reducing the sensory weight in the Kalman

235   gain, the controller becomes less sensitive to sensory information. This is due to the uncertainty induced

236   by the motor commands, which in this case it is clearly independent of the retinal image. The

237   contribution of our model is to show that this stimulus-independent reduction in response gain may be

238   rooted in efficient computations about the state of the eye.

239   We propose such a mechanism as plausible origin of saccadic suppression, but cannot indicate

240   how the visual system performs this operation at the level of neural circuits. We draw a qualitative link

241   between Kalman filtering and the reduction in sensory weight or neural excitability, and thus this link

242   remains speculative. However, the model does provide hints about what to look for. First, the increase in

243   extrapolation variance clearly results from convolving the motor-dependent noise with the expected eye

244   dynamics over the delay interval. Second, this increase is directly proportional to the integrated motor

245   command. Thus, convolutional networks in the visual system receiving the corollary discharge as input

246   may easily implement a reduction in the gain of neural responses that achieves statistically optimal

247   sensory weighting. Any anatomical or functional similarity between these putative neural operations and

248   neural data may thus provide insight into the circuitry underlying state estimation.

249   Besides these limitations, we believe that the model is compelling because it is simple. The

250   insight behind our model was to consider both sensory delays and noisy commands together, which are

251   known to play an important role in sensorimotor control [49,50]. Our approach combines predictive control

252   (based in this case on *finite-spectrum assignment* [51]) and optimal filtering [52], to derive a closed-loop

253   controller that handles delays and noise efficiently. In this framework, the weight of feedback must be

254   adjusted not due to movement on its own, but to the uncertainty that results from motor noise and

255   sensory delays. This result, and the diversity of behaviors that the model reproduces, simply fell out of

256   the simplest instance of stochastic optimal control (LQG).

257   In addition to reproducing saccadic suppression, our model succeeded at the difficult task of

258 controlling fast movements with comparatively long delays, without artificially interrupting the sensory

259 inflow. Indeed, previous models of saccadic control tend to only consider *open-loop* controllers [49], or

260 closed-loop control with internal feedback only [25,53,54], while it is clear that sensory information remains

261 available and may influence online control [27,28]. Here our model predicts that sensory feedback must be

262 strongly reduced, but not completely suppressed, as observed experimentally [18]. This is because the

263 Kalman filter achieves an optimal projection in the probabilistic sense, by making the estimation error

264 orthogonal to (or statistically uncorrelated with) the estimated state. Thus, the decrease in the Kalman

265 gain during movement indicates that state information prior to the saccade still carries some information

266 about the current state, and thus can be exploited to derive optimal estimates. The resulting control law

267 (see Methods, Eqn. 10) plays the role of a burst generator, and can be easily inserted as such in more

268 complex models of gaze control.

269   Perception and control may thus share a common neural substrate in the visual system. The

270 question of why the nervous system shares resources remains open. If perceptual and sensorimotor

271 processes were completely decoupled, we could perform better (Fig. 1, H1). Thus the hypothesis of

272 shared resources must find a good reason to live (Fig. 1, H2). First it is clear that the corollary discharge is

273 critical to monitor the consequences of motor commands. Thus, perception is already conditional upon

274 the ability to integrate extra-retinal signals accurately, both during saccade and pursuit [24,32,40,55]. Second,

275 although perception on its own is suboptimal during saccades (we discard a lot of meaningful

276 information), the shared resources model is clearly cheaper in terms of neural resources. It may thus be

277 globally optimal if the perceptual loss is not more penalizing than the cost of dedicating more neural

278 resources to visual processing in general, considering perceptual and control systems together. Using the

279 same posterior belief for perception and action also ensures self-consistency, in the sense that the same

280 stimulus is not deemed more or less reliable dependent on how we use it. Self-consistency is known to

281   characterize perceptual judgment tasks, where participants make a continuous use of the hypothesis

282   that they previously committed to [56]. Our model suggests that similar principles may governs the use of

283   posterior beliefs about the state of the eye for perception and control, indicating that these functions

284   emerge from a shared neural substrate. We expect that future work investigate whether this theory is

285   generally applicable to other examples of active sensory suppression associated with voluntary actions

286   such as force generation or reaching[57-59].

287

288   **Methods**

289   *Biomechanical model*

290   We consider a second-order, low-pass filter as a biomechanical model of the oculomotor plant.

291   Based on previous modeling work [60] we set the time constants to $\tau_1 = 224ms$ and $\tau_2 = 13ms$. In the

292   sequel, scalars are represented with lower-case characters, vectors with bold lower-case and matrices

293   with capitals. Thus the state-space representation of the continuous-time differential equation

294   representing the eye dynamics was:

295   (1) $$\begin{bmatrix} \dot{x}_1 \\ \dot{x}_2 \end{bmatrix} = \begin{bmatrix} 0 & 1 \\ -1/(\tau_1\tau_2) & -(\tau_1+\tau_2)/(\tau_1\tau_2) \end{bmatrix}\begin{bmatrix} x_1 \\ x_2 \end{bmatrix} + \begin{bmatrix} 0 \\ 1/(\tau_1\tau_2) \end{bmatrix}u,$$

296   where x_1 is the eye angle, x_2 is the eye velocity, u is the command input and the dot operator is the time

297   derivative. The explicit dependency on time was omitted for clarity. This representation takes the form:

298   (2) $\dot{x} = Ax + Bu,$

299   with $x := [x_1 \ x_2]^T$ representing the state of the system.

300   The plant model was then augmented with the target position and target velocity, and

301   transformed into discrete time model to include sensorimotor noise. The discrete-time stochastic

302   dynamics and the measurement equations are as follows:

303   (3) $x(t + dt) = A_d x(t) + B_d u(t) + \alpha\varepsilon_t B_d u(t) + \xi_t,$

304   (4) $y(t) = x(t - \delta t) + \sigma_t.$

305   The matrices A_d and B_d form the discrete-time state space representation of the continuous-time

306   system defined in Eqn. 1, which for a discretization step of dt corresponds to: $A_d = e^{dtA}$, and

307    $B_d = \left(\int_0^{dt} e^{sA}ds\right)B$. The constant $\alpha > 0$ is a scaling parameter; ε_t, ξ_t and σ_t are Gaussian noise

308   disturbances. The multiplicative noise (ε_t) is a scalar with zero mean and unit variance, whereas the

309   additive sources of noise are 4-dimensional random disturbances with zero mean and variance set to

310    $\Sigma_{\xi,\sigma}$, which will be defined below (recall that the state vector includes that target position and velocity).

15

311   The measurement delay was $\delta t = 100 ms$ in a agreement with measured and modeled latencies of rapid

312   saccadic responses to visual stimuli [61,62]. The subscript t for the random noise disturbances was used to

313   remind that these series do not have finite instantaneous variation; but they have finite variance over

314   the discretization interval of dt.

315

316   *Closed-loop controller*

317   Optimal estimation and control of the stochastic system defined in Eqns. 3 and 4 can be derived

318   in the framework of extended Linear-Quadratic-Gaussian control (LQG), including the effect of control

319   and state-dependent noise [63]. However this approach is not necessarily well suited for handling

320   sensorimotor delays because it requires system augmentation [35], and as a consequence the estimator

321   achieves optimal (probabilistic) projection of the prior estimate onto the delayed state measurement [52].

322   Since we know that the visual system extrapolates sensory information to compute the present state of

323   the eye or of a moving target [29-31,64], we were interested to derive an optimal estimator that explicitly

324   extrapolates sensory signals, captured in $y(t)$, over the interval δt (see also Fig. 2). The key aspect of this

325   estimator design is that, by taking into account the control function $u(s), t - \delta t \le s \le t$, the variance of

326   the extrapolated sensory signal is dynamically adjusted as a function of the control-dependent noise (3rd

327   term of Eqn. 3).

328   More precisely, we assume that neural processing of sensory signals consists in computing an

329   estimate of the present state of the eye given the delayed sensory signals as follows:

$$x(t|y) = e^{\delta t A} y(t) + \int_{t-\delta t}^{t} e^{(t-s)A} B u(s) ds.$$

330   (5)

331   Using the notation $M(t) := e^{tA}$, it is easy to observe that the extrapolation error (Δ_t) follows a Gaussian

332   distribution defined as follows:

333   (6) $x(t|y) = x(t) + \Delta_t,$

16

334   (7) $\mathbf{\Delta}_t \sim N(0, V_t),$

$$V_t = M(\delta t)\Sigma_\sigma M(\delta t)^T + \int_{t-\delta t}^{t} \alpha'^2 M(t-s)Bu(s)u(s)^T B^T M(t-s)^T ds,$$

335   (8)

336   where $\alpha' := \alpha(dt)^{-1/2}$ was defined in agreement with the unit-variance Brownian noise disturbance

337   considered for the stochastic differential equation.

338   With these definitions, we can derive an adaptive estimator based on standard Kalman filtering

339   using the extrapolated state (Eqn. 8) instead of the available state measurement (Eqn. 4). The state

340   estimate is computed in two steps as follows:

341   (9) $\hat{\mathbf{x}}^P(t+dt) = A_d \hat{\mathbf{x}}(t) + B_d u(t),$

342   (10) $\hat{\mathbf{x}}(t+dt) = \hat{\mathbf{x}}^P(t+dt) + K(t)\big(\mathbf{x}(t|\mathbf{y}) - \hat{\mathbf{x}}(t)\big),$

343   and the Kalman gain, $K(t)$, as well as the covariance of the estimated state are updated iteratively

344   following standard procedures [52].

345   Observe that the separation principle does not hold because the variances of the one-step

346   prediction and of $\mathbf{\Delta}_t$ both depend on u_t. Thus our approach is valid under the assumption that the

347   control must not be jointly optimized with the state estimator. Instead of optimizing iteratively the

348   controller and the state estimator as in the extended LQG framework [63,65], we computed the controller

349   independently based on the heuristic assumption that the separation principle applied, and then

350   optimized the state estimator defined in Eqns. 9-10 by taking into account the effect of control-

351   dependent noise explicitly (Eqns. 6-8). The controller was thus obtained by solving the LQG control

352   problem while ignoring the multiplicative noise in Equation 3 as follows:

353   (10) $u(t) = \big(R + B_d^T S_{t+1} B_d\big)^{-1} B_d^T S_{t+1} A \hat{\mathbf{x}}(t).$

354   In Eqn. 10, R represents the cost of motor commands, and the matrices S_t are computed offline

355   following standard procedures [63,66].

17

356   We developed this approach to include the extrapolation of sensory data while considering the

357   control over the delay interval explicitly. Using feedback control based on a predicted state is known as

358   *finite spectrum assignment* (FSA), which is germane to a Smith predictor in that it aims at removing the

359   delay from the feedback loop [51]. Here, FSA was chosen to reconstruct the predicted state (instead of the

360   system output as for the Smith predictor), allowing the use of position and velocity estimates in the

361   control law (Eqn. 10).

362

363   *Numerical Simulations*

364   The only free parameters are α (the scaling of the signal dependent noise), the covariance

365   matrices of $\boldsymbol{\xi}_t$ and $\boldsymbol{\sigma}_t$ (respectively Σ_{ξ} and Σ_{σ}), and the cost-function used for control. We used the

366   following values: the constant α was set to 0.08, Σ_{ξ} was $10^{-3} \times B_d B_d^T$ and Σ_{σ} was 10^{-6} times the

367   identity matrix of appropriate dimension. These parameters were manually adjusted so that when

368   adding the signal-dependent term to the variance of the extrapolation error (Eqn. 8), the Kalman gains

369   converged to steady-state values and the variances of the extrapolated state and of the motor noise

370   were comparable during fixation. It is clear that changing the noise parameters may influence the results

371   qualitatively. However the key feature of the adaptive estimator is that the extrapolation variance

372   increases monotonically with the square of the motor command, which is why the extrapolated

373   measurement is dynamically reduced during movement. This aspect does not depend on the different

374   noise parameters.

375   The cost parameters were adjusted to generate simulated saccades compatible with typical

376   recordings of eye movements in humans, and these parameters do not impact the results qualitatively.

377   For saccadic movements, we simulated two fixation periods at the initial (x_1^*) and final (x_2^*) targets during

378   which the cost of position error was $Q_{FIXATION,i} = (x_1 - x_i^*)^2$. The two fixation periods were separated

379   by the movement time, which was a 50ms window during which the eye was free to move without any

18

380   penalty on the state vector. For the smooth movements in response to velocity jumps, we simulated a

381   fixation to the target and changed the target state during a simulation run. The cost of motor commands

382   in all cases was $Ru(t)^2$, with $R := 0.01$. Finally we used a discretization step of 5ms.

383   One difficulty is that the extrapolation requires that all state variables, including the target, be

384   observed independently (Eqn. 4). This is not fully compatible with the visual system, because there is no

385   measurement of the target state independent of the state of the eye. This limitation could be overcome

386   by considering another observer that reconstructs the state vector prior to extrapolating the sensory

387   feedback. Here, instead of considering such additional observer, we injected similar amounts of signal-

388   dependent noise in the sensory feedback about the state of the eye as about the state of the target. This

389   procedure was chosen for simplicity and captures the intuitive idea that if the eye position is very noisy,

390   then information about the target location logically shares the same uncertainty.

Figure Legends

Figure 1. Schematic illustration of two hypotehses. The sensory input, $y(.)$ is a function of the variable of interest, x. The posterior distribution of x is represented by $P(x)$. The estimate of x is designated by $\hat{x}$, which can be any statistics related to $P(x)$ such as the posterior mean or mode. Finally the control command is a function of the estimate, represented by $u(\hat{x})$. In the hypothesis of separated resources (H1), computations of the posterior belief are carried out independently for perception and control. In this scenario, the uncertainty induced by the control commands does not impact the perceptual estimate. This possible architecture is optimal in the sense that it would minimize loss of sensory information. In the hypothesis of shared resource (H2), the computation of the posterior belief about the state of a variable is shared for perception and control, thus both processes are similarly influenced by control-dependent noise. Although the first hypothesis is optimal, the second hypothesis is more efficient in terms of neural resources, and is also self-consistent (see Discussion).

Figure 2. a. Schematic representation of the control and estimation architectures. We consider a closed loop controller based on optimal feedback control and state estimation. The dynamics of the eye plant corresponded to a second order system with time constants taken from the literature (13ms and 224ms). Bottom: Optimal state estimator based on usual Kalman filtering, and augmented with the extrapolation of sensory feedback to compensate for sensorimotor delays (Sensory Extrapolation, red box). The symbolic representation of the signals in blue follows the same notations as in the Methods: $y(t)$ is the sensory feedback, $\hat{x}(t|y)$ is the extrapolation of sensory feedback, $u(.)$ is the sequence of previous and current control commands, $\hat{x}^P(.)$ and $\hat{x}(.)$ are the prior and posterior estimates at the corresponding time steps. **b.** Top: Modeled saccadic eye movement from the first (x_1^*) to the second fixation target (x_2^*). Bottom: Associated control function. Time zero corresponds to the end of the fixation period to the first target. **c.** Illustration of the sensory extrapolation performed in the state estimator. The simulated task is

20

415   to track the target, which suddenly starts moving (velocity jump) with or without position jump in the

416   opposite direction. The simulated eye trajectory shows how the extrapolation of target motion over the

417   delay interval generates a catch up saccade (black arrow). This compensatory movement is also

418   illustrated in the velocity trace.

419

420   **Figure 3. a.** Variance of the control signal (solid) and of the extrapolation of sensory feedback (dashed).

421   Four times are represented to illustrate how signal-dependent noise impacts the extrapolation of

422   sensory feedback is (t_1 = -100ms, t_2 = -50ms, t_3 = 0ms, and t_4 = 50ms). The dots with similar color

423   represent the moment when the information at the corresponding time is available ($t_i + 100ms$).

424   Observe the increase in extrapolation variance associated with stimuli between t_1 and t_2. **b.** Weight of

425   the position feedback for correcting the estimate of the position. This weight is directly taken from the

426   Kalman gain matrix. The reduction in Kalman gain at each selected time point is directly linked to the

427   increase in variance. **c.** Representation of a modeled saccadic eye movement, with the gray area

428   corresponding to the interval of time during which sensory input is given less weight as a result of the

429   extrapolation variance. **d.** Control and extrapolation variance normalized to the maximum values

430   obtained for saccades of 20deg (top traces). **e.** Weight of sensory feedback for the two simulations.

431   Observe that although the catch-up saccade is very small (~2deg), the transient increase in extrapolation

432   variance gives rise to a reduction in weight. **f.** Illustration of the smooth pursuit task with (dark blue) or

433   without (light blue) initial target jump occurring simultaneously with the velocity jump. The absence of

434   target jump evokes a catch-up saccade, which is associated with ta reduction in sensory weight. There is

435   no reduction with the initiation of smooth pursuit.

436

437   **Figure 4.** Representation of a simulated 20deg saccade ad dynamic weight of sensory feedback, with the

438   perisaccadic suppression highlighted in gray. These traces are similar as Figure 3a and 3c. The images

21

439   represent the convolution of a horizontal stripe with a Gaussian kernel with variance proportional to the

440   extrapolation variance to highlight that assigning higher variance may lead to reduced contrast, even

441   when the movement is aligned with the stimulus orientation. Times correspond to the Fig. 3. The

442   decrease in Kalman gain occurs from 0 to 150ms relative to saccade onset (solid trace: time locked), thus

443   the window during which stimuli are suppressed corresponds to -100 to 50ms (dashed trace: stimulus-

444   locked). **b.** Illustration of how the predicted saccadic suppression compares with previously reported

445   suppression from behavioral and neural data. The duration of the perisaccadic suppression in the model

446   is the sum of the temporal delay and of the movement time as represented above with the gray

447   rectangle. Comparisons are approximate as movement time was not the same across all studies. The

448   solid and dashed traces for saccadic suppression in SC indicates the range of onset and offset as given by

449   Hafed and Krauzlis[40]. Other intervals of saccadic suppression were drawn following the authors'

450   summary or based on visual inspection of the corresponding references.

451

References

1   Kording, K. Decision theory: What "should" the nervous system do? *Science* **318**, 606-610 (2007).

2   Angelaki, D. E., Gu, Y. & DeAngelis, G. C. Multisensory integration: psychophysics, neurophysiology, and computation. *Current Opinion in Neurobiology* **19**, 252-258 (2009).

3   Ernst, M. O. & Banks, M. S. Humans integrate visual and haptic information in a statistically optimal fashion. *Nature* **415**, 429-433 (2002).

4   van Beers, R. J., Sittig, A. C. & van der Gon, J. J. D. Integration of proprioceptive and visual position-information: An experimentally supported model. *Journal of Neurophysiology* **81**, 1355-1364 (1999).

5   Fetsch, C. R., Pouget, A., DeAngelis, G. C. & Angelaki, D. E. Neural correlates of reliability-based cue weighting during multisensory integration. *Nat Neurosci* **15**, 146-154 (2012).

6   Drugowitsch, J., DeAngelis, G. C., Klier, E. M., Angelaki, D. E. & Pouget, A. Optimal multisensory decision-making in a reaction-time task. *Elife* **3** (2014).

7   Acuna, D. E., Berniker, M., Fernandes, H. L. & Kording, K. P. Using psychophysics to ask if the brain samples or maximizes. *J Vis* **15** (2015).

8   Wolpert, D. M., Ghahramani, Z. & Jordan, M. I. An internal model for sensorimotor integration. *Science* **269**, 1880-1882 (1995).

9   Kording, K. P. & Wolpert, D. M. Bayesian integration in sensorimotor learning. *Nature* **427**, 244-247 (2004).

10   Izawa, J. & Shadmehr, R. On-Line Processing of Uncertain Information in Visuomotor Control. *Journal of Neuroscience* **28**, 11360-11368 (2008).

11   Crevecoeur, F., Munoz, D. P. & Scott, S. H. Dynamic Multisensory Integration: Somatosensory Speed Trumps Visual Accuracy during Feedback Control. *J Neurosci* **36**, 8598-8611 (2016).

12   Cisek, P. Making decisions through a distributed consensus. *Current Opinion in Neurobiology* **22** (2012).

13   Wolpert, D. M. & Landy, M. S. Motor control is decision making. *Current Opinion in Neurobiology* (2012).

14   Wurtz, R. H. Neuronal mechanisms of visual stability. *Vision Res* **48**, 2070-2089 (2008).

15   Ibbotson, M. & Krekelberg, B. Visual perception and saccadic eye movements. *Curr Opin Neurobiol* **21** (2011).

16   Diamond, M. R., Ross, J. & Morrone, M. C. Extraretinal control of saccadic suppression. *J Neurosci* **20**, 3449-3455 (2000).

17   Thiele, A., Henning, P., Kubischik, M. & Hoffmann, K. P. Neural mechanisms of saccadic suppression. *Science* **295**, 2460-2462 (2002).

18   Castet, E. & Masson, G. S. Motion perception during saccadic eye movements. *Nat Neurosci* **3**, 177-183 (2000).

19   Burr, D. C., Morrone, M. C. & Ross, J. Selective suppression of the magnocellular visual pathway during saccadic eye movements. *Nature* **371**, 511-513 (1994).

20   Burr, D. C., Morgan, M. J. & Morrone, M. C. Saccadic suppression precedes visual motion analysis. *Curr Biol* **9**, 1207-1209 (1999).

21   Van Gisbergen, J. A., Robinson, D. A. & Gielen, S. A quantitative analysis of generation of saccadic eye movements by burst neurons. *J Neurophysiol* **45**, 417-442 (1981).

22   Goossens, H. H. & Van Opstal, A. J. Blink-perturbed saccades in monkey. I. Behavioral analysis. *J Neurophysiol* **83**, 3411-3429 (2000).

23   Xu-Wilson, M., Tian, J., Shadmehr, R. & Zee, D. S. TMS perturbs saccade trajectories and unmasks an internal feedback controller for saccades. *J Neurosci* **31**, 11537-11546 (2011).

498 24 Sommer, M. A. & Wurtz, R. H. Visual perception and corollary discharge. *Perception* **37**, 408-418
499   (2008).
500 25 Optican, L. M. in *Encyclopedia of Neuroscience* Vol. 7 (ed L R Squire) 25-34 (Oxford: Academic
501   Press, 2009).
502 26 Burr, D. C. & Morrone, M. C. Temporal impulse response functions for luminance and colour
503   during saccades. *Vision Res* **36**, 2069-2078 (1996).
504 27 Gaveau, V. *et al.* On-line modification of saccadic eye movements by retinal signals. *Neuroreport*
505   **14**, 875-878 (2003).
506 28 West, G. L., Welsh, T. N. & Pratt, J. Saccadic trajectories receive online correction: evidence for a
507   feedback-based system of oculomotor control. *J Mot Behav* **41**, 117-127 (2009).
508 29 Bennett, S. J., de Xivry, J.-J. O., Barnes, G. R. & Lefevre, P. Target acceleration can be extracted
509   and represented within the predictive drive to ocular pursuit. *Journal of Neurophysiology* **98**,
510   1405-1414 (2007).
511 30 Ferrera, V. P. & Barborica, A. Internally generated error signals in monkey frontal eye field during
512   an inferred motion task. *J Neurosci* **30**, 11612-11623 (2010).
513 31 Diaz, G., Cooper, J., Rothkopf, C. & Hayhoe, M. Saccades to future ball location reveal memory-
514   based prediction in a virtual-reality interception task. *J Vis* **13** (2013).
515 32 Blohm, G., Missal, M. & Lefevre, P. Processing of retinal and extraretinal signals for memory-
516   guided saccades during smooth pursuit. *Journal of Neurophysiology* **93**, 1510-1522 (2005).
517 33 de Brouwer, S., Yuksel, D., Blohm, G., Missal, M. & Lefevre, P. What triggers catch-up saccades
518   during visual tracking? *J Neurophysiol* **87**, 1646-1650 (2002).
519 34 Todorov, E. & Jordan, M. I. Optimal feedback control as a theory of motor coordination. *Nature*
520   *Neuroscience* **5**, 1226-1235 (2002).
521 35 Crevecoeur, F. & Scott, S. H. Priors Engaged in Long-Latency Responses to Mechanical
522   Perturbations Suggest a Rapid Update in State Estimation. *Plos Computational Biology* **9** (2013).
523 36 Orban de Xivry, J. J. & Lefevre, P. Saccades and pursuit: two outcomes of a single sensorimotor
524   process. *J Physiol* **584**, 11-23 (2007).
525 37 Krauzlis, R. J. Recasting the smooth pursuit eye movement system. *J Neurophysiol* **91**, 591-603
526   (2004).
527 38 Rashbass, C. The relationship between saccadic and smooth tracking eye movements. *J Physiol*
528   **159**, 326-338 (1961).
529 39 Schutz, A. C., Braun, D. I. & Gegenfurtner, K. R. Contrast sensitivity during the initiation of
530   smooth pursuit eye movements. *Vision Res* **47**, 2767-2777 (2007).
531 40 Hafed, Z. M. & Krauzlis, J. in *Dynamics of Visual Motion Processing: Neural Behavioral, and*
532   *Computatiional Approaches*   (eds U J Ilg & G S Masson) 189-211 (Springer, 2010).
533 41 Watson, T. & Krekelberg, B. An equivalent noise investigation of saccadic suppression. *J Neurosci*
534   **31**, 6535-6541 (2011).
535 42 Bridgeman, B., Hendry, D. & Stark, L. Failure to detect displacement of the visual world during
536   saccadic eye movements. *Vision Res* **15**, 719-722 (1975).
537 43 Beeler, G. W., Jr. Visual threshold changes resulting from spontaneous saccadic eye movements.
538   *Vision Res* **7**, 769-775 (1967).
539 44 Ridder, W. H. & Tomlinson, A. A comparison of saccadic and blink suppression in normal
540   observers. *Vision Research* **37**, 3171-3179 (1997).
541 45 Ibbotson, M. R., Crowder, N. A., Cloherty, S. L., Price, N. S. & Mustari, M. J. Saccadic modulation
542   of neural responses: possible roles in saccadic suppression, enhancement, and time
543   compression. *J Neurosci* **28**, 10952-10960 (2008).
544 46 Reppas, J. B., Usrey, W. M. & Reid, R. C. Saccadic eye movements modulate visual responses in
545   the lateral geniculate nucleus. *Neuron* **35**, 961-974 (2002).

546   47   Kagan, I., Gur, M. & Snodderly, D. M. Saccades and drifts differentially modulate neuronal
547   activity in V1: effects of retinal image motion, position, and extraretinal influences. *J Vis* **8**, 19 11-
548   25 (2008).
549   48   Bremmer, F., Kubischik, M., Hoffmann, K. P. & Krekelberg, B. Neural dynamics of saccadic
550   suppression. *J Neurosci* **29**, 12374-12383 (2009).
551   49   Harris, C. M. & Wolpert, D. M. Signal-dependent noise determines motor planning. *Nature* **394**,
552   780-784 (1998).
553   50   Miall, R. C., Weir, D. J., Wolpert, D. M. & Stein, J. F. Is the Cerebellum a Smith Predictor ? *Journal*
554   *of Motor Behavior* **25**, 203-216 (1993).
555   51   Zhong, Q. C. *Robust Control of Time-delay Systems*. (Spinger-Verlag, 2010).
556   52   Anderson, B. D. O. & Moore, J. D. *Optimal Filtering*. (Prentice-Hall, 1979).
557   53   Jurgens, R., Becker, W. & Kornhuber, H. H. Natural and drug-induced variations of velocity and
558   duration of human saccadic eye movements: evidence for a control of the neural pulse generator
559   by local feedback. *Biol Cybern* **39**, 87-96 (1981).
560   54   Chen-Harris, H., Joiner, W. M., Ethier, V., Zee, D. S. & Shadmehr, R. Adaptive control of saccades
561   via internal feedback. *J Neurosci* **28**, 2804-2813 (2008).
562   55   Bedell, H. E. & Lott, L. A. Suppression of motion-produced smear during smooth pursuit eye
563   movements. *Curr Biol* **6**, 1032-1034 (1996).
564   56   Stocker, A. A. & Simoncelli, E. P. A Bayesian Model of Conditioned Perception. *Adv Neural Inf*
565   *Process Syst* **2007**, 1409-1416 (2007).
566   57   Chapman, C. E., Bushnell, M. C., Miron, D., Duncan, G. H. & Lund, J. P. Sensory perception during
567   movement in man. *Exp Brain Res* **68**, 516-524 (1987).
568   58   Blakemore, S. J., Frith, C. D. & Wolpert, D. M. Spatio-temporal prediction modulates the
569   perception of self-produced stimuli. *J Cogn Neurosci* **11**, 551-559 (1999).
570   59   Seki, K., Perlmutter, S. I. & Fetz, E. E. Sensory input to primate spinal cord is presynaptically
571   inhibited during voluntary movement. *Nature Neuroscience* **6**, 1309-1316 (2003).
572   60   Robinson, D. A., Gordon, J. L. & Gordon, S. E. A model of the smooth pursuit eye movement
573   system. *Biol Cybern* **55**, 43-57 (1986).
574   61   Munoz, D. P. & Everling, S. Look away: The anti-saccade task and the voluntary control of eye
575   movement. *Nature Reviews Neuroscience* **5**, 218-228 (2004).
576   62   Stanford, T. R., Shankar, S., Massoglia, D. P., Costello, M. G. & Salinas, E. Perceptual decision
577   making in less than 30 milliseconds. *Nature Neuroscience* **13**, 379-U326 (2010).
578   63   Todorov, E. Stochastic optimal control and estimation methods adapted to the noise
579   characteristics of the sensorimotor system. *Neural Computation* **17**, 1084-1108 (2005).
580   64   Blohm, G., Missal, M. & Lefevre, P. Processing of retinal and extraretinal signals for memory-
581   guided saccades during smooth pursuit. *J Neurophysiol* **93**, 1510-1522 (2005).
582   65   Phillis, Y. A. Controller Design of Systems with Multiplicative Noise. *Ieee Transactions on*
583   *Automatic Control* **AC-30**, 1017-1019 (1985).
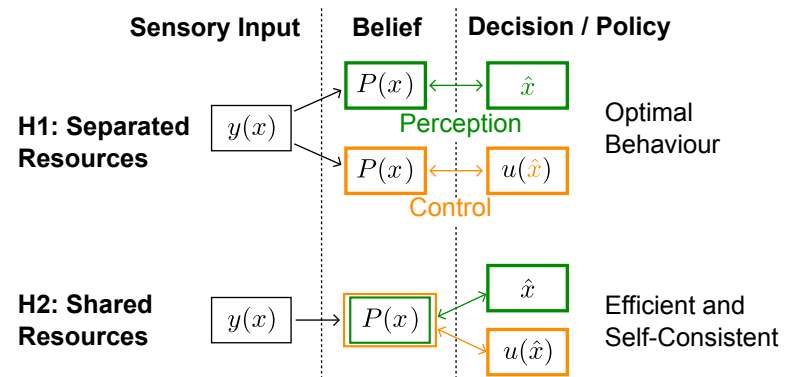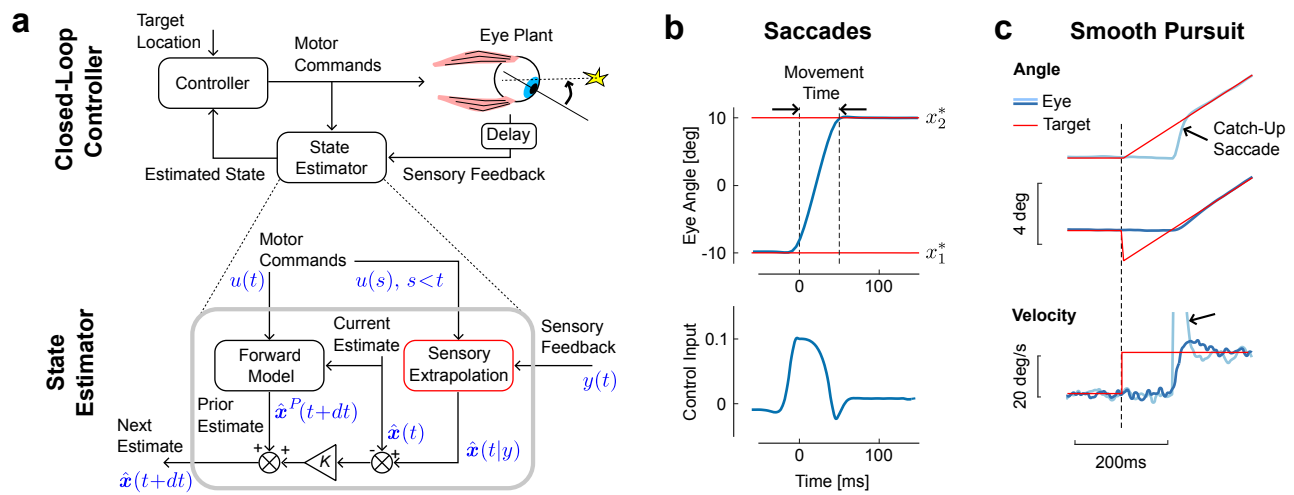584   66   Astrom, K. J. *Introduction to stochastic control theory*. (Academic Press, 1970).
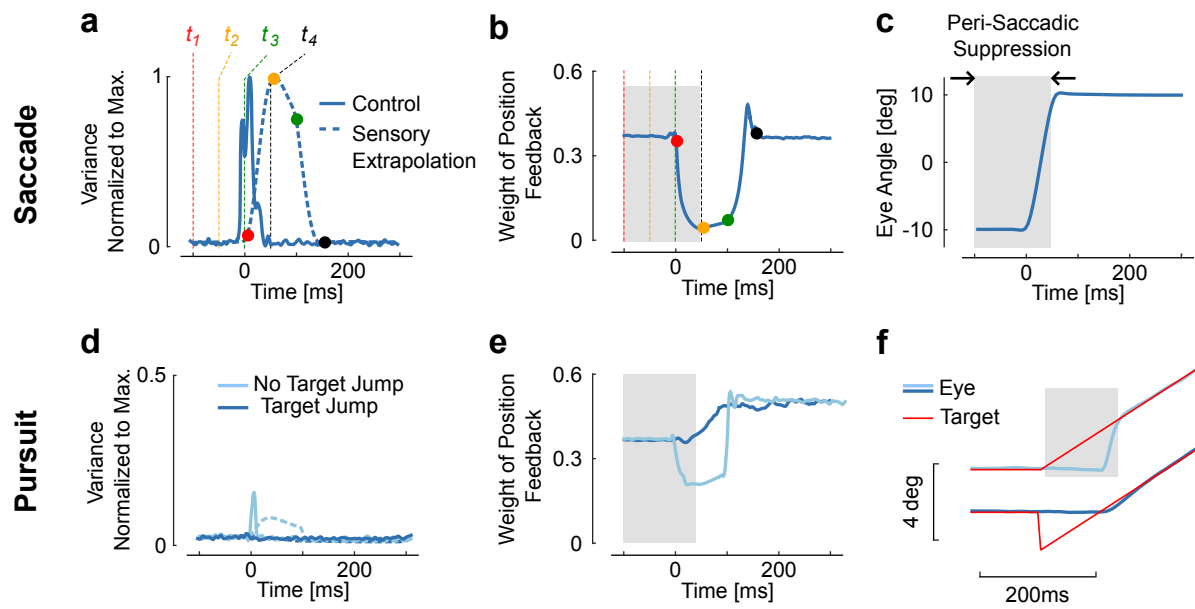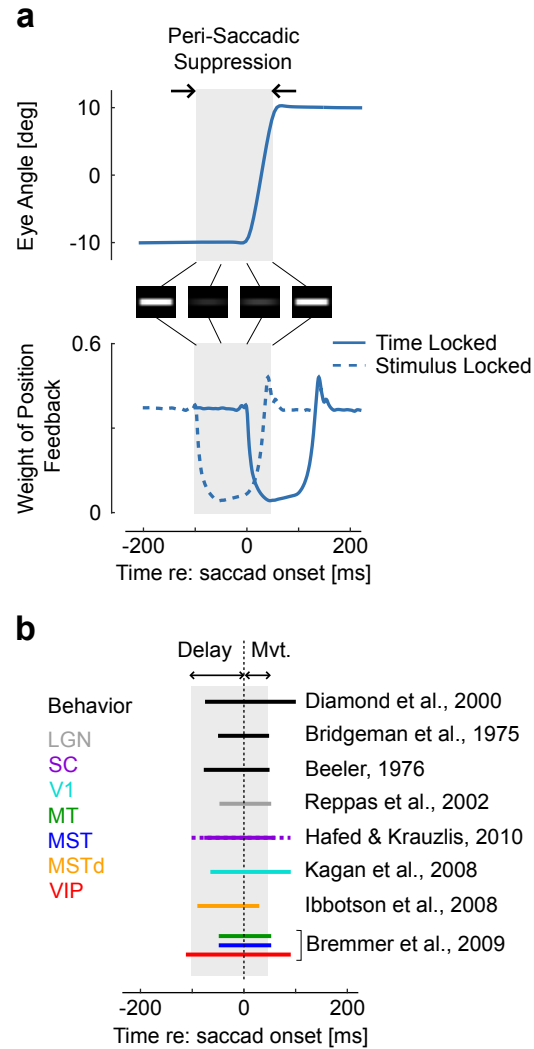
Figure 1

Figure 2

Figure 3

Figure 4